Chapter 3. Velocity Estimation in a Nearly Stratified Earth

The previous chapter showed that ellipses in slant frames replace hyperbolas in standard coordinates, and indicated that a parallel velocity estimation scheme can be developed for a layered media earth model. We will demonstrate in this chapter that this is indeed the case.

In addition, while allowing the velocity to be a function only of depth, we will relax somewhat the restriction of zero dip reflectors. In standard coordinates, the transformation to a common midpoint coordinate frame effects a first order dip correction. In slant frames, a first order dip correction is effected by a transformation to interpretation coordinates. These were defined in Chapter 2 and are derived for the case of a depth-dependent velocity in this chapter.

A Root Mean Square Velocity Theorem for Slant Frames

Dix (1955) showed that with the assumption of straight line ray paths in the subsurface and the acoustic velocity a function only of depth, that in the case of horizontal reflectors a velocity estimation procedure which looks for coherence along hyperbolics will yield a root mean square velocity. That is, if the trajectory of a single event is assumed to be of the form

$$t^2 = t_0^2 + \frac{f^2}{\bar{v}^2} \tag{3.1}$$

with $\bar{v}$ some constant, then provided all ray paths are straight,

$$\bar{v}^2 = \frac{1}{t_0} \int_0^{t_0} v^2(t_0)\, dt_0 \equiv v_{rms}^2 \tag{3.2}$$

where the integral is done over a vertical ray path. Since we cannot expect perfectly straight ray paths for any but infinitesimal offsets, the straight line ray path approximation is also known as the small offset approximation.

As in the previous chapter, the coordinate t_0 is the two-way vertical travel time to a reflector at depth, z. We generalize it here to a depth-dependent velocity.

$$t_0 \equiv 2 \int_0^z \frac{dz}{v(z)} \tag{3.3}$$

or, conversely if we re-express the velocity at some depth as a function of the variable, t_0, that is, if

$$v(z) = v'(t_0)$$

then

$$z = \frac{1}{2} \int_0^{t_0} v'(t_0)\, d\, t_0 \tag{3.4}$$

In subsequent derivations, the primes on functions of t_0 will be dropped to simplify notation.

We shall now derive a root mean square velocity theorem for slant frames using only the straight line ray path approximation. Figure 2.8 shows the basic geometry of the slant frame. The stack has been done over some fixed ray parameter, p, giving us a plane wave at constant θ for velocity constant. In the case of a depth-variable velocity, the stacking parameter, p, will remain a constant for a single ray path. The slant frame time coordinate, t', is defined by

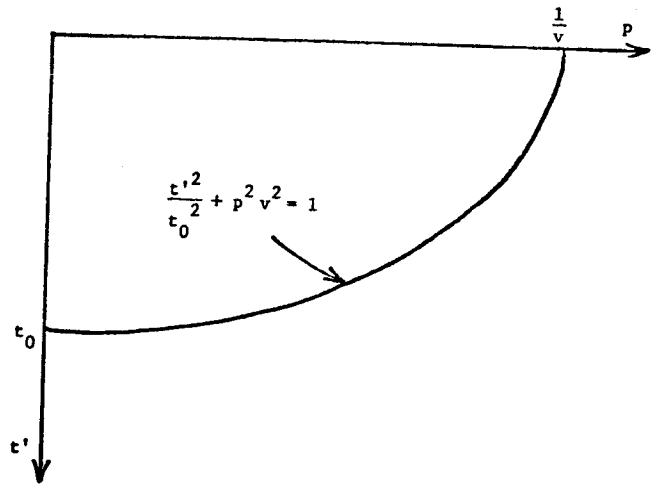

Figure 3.1. The travel time curve showing t' versus p for a constant velocity medium. The intercept at $p=0$ is $t' = t_0$, where t_0 maintains the same meaning as in CDP geometry: the two-way vertical travel time. The intercept at $t' = 0$ is $p = 1/v$, where v is the (constant) material velocity. The "family" of elliptical travel time curves for many reflectors all have the same intercept at $t' = 0$, but have a unique intercept at $p=0$.

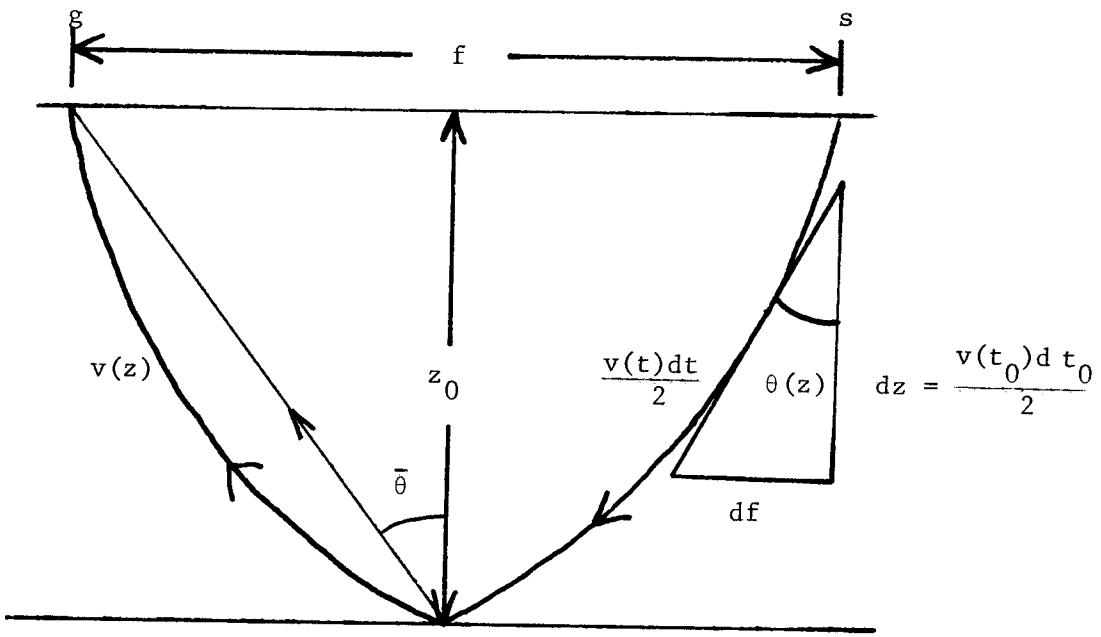

Figure 3.2. A possible ray path for a more realistic velocity which is a function of z. The small triangle relates some important differentials at depth, z. The straight upcoming path represents the straight line ray path assumption.

$$t' = t - f\,p \tag{3.5}$$

Now for a constant velocity medium, we recall the following equation from Chapter 2.

$$\frac{t'}{t_0} = \frac{t_0}{t} = \cos\theta = (1 - p^2 v^2)^{1/2} \tag{2.9}$$

Figure 3.2 shows a ray path in a depth-variable velocity medium. We make the assumption of a straight line ray path at some angle $\bar{\theta}$ in the figure, and write

$$\frac{t'}{t_0} = \frac{t_0}{t} = \cos\bar{\theta} = (1 - p^2 \bar{v}^2)^{1/2} \tag{3.6}$$

An equation like (3.6) was derived for a constant velocity medium, and we can expect the trajectory of an event in (p,t') space to follow this functional dependence only in that case. However, if we force the trajectory of an event in a depth-variable velocity medium to follow the form of (3.6), then of course we will find that $\bar{v}$ will be a function of p. Making the claim of a straight line ray path is equivalent to specifying $\bar{v}$ to be a constant. However, by forcing $\bar{v}$ to be constant we will find that (3.6) describes our event closely only when the offset f is small (or equivalently, when p is small), and thus is also called the small offset approximation.

We now rewrite (3.6) in the form

$$\frac{t'}{t} = \cos^2\bar{\theta} = 1 - p^2 \bar{v}^2 \tag{3.7}$$

and combine it with (3.5) to obtain

$$\frac{t - f\,p}{t} = 1 - p^2\,\bar{v}^2$$

or

$$-\frac{f\,p}{t} = -\,p^2\,\bar{v}^2$$

or

$$\bar{v}^2 = \frac{f}{p\,t} \tag{3.8}$$

Observing Figure 3.2 again shows that we can express the offset as

$$f = 2\int_0^z \tan\theta(z)\,dz \tag{3.9}$$

or, using the transformation of (3.4),

$$f = \int_0^{t_0} v(t_0)\,\tan\theta(t_0)\,d\,t_0$$

$$= \int_0^{t_0} \frac{p\,v^2(t_0)\,d\,t_0}{(1-p^2v^2(t_0))^{1/2}} \tag{3.10}$$

Note that in expression (3.10) the denominator changes more slowly with a change in v than does the numerator if $p \ll 1$. Since we are using the small offset approximation, we take the denominator outside the integral.

$$f \cong \frac{p}{(1-p^2\bar{v}^2)^{1/2}} \int_0^{t_0} v^2(t_0)\,d\,t_0$$

$$\cong \frac{p}{\cos\bar{\theta}} \int_0^{t_0} v^2(t_0)\,d\,t_0 \tag{3.11}$$

which, when combined with (3.8) gives

$$\bar{v}^2 \cong \frac{1}{t \cos \bar{\theta}} \int_0^{t_0} v^2(t_0)\, d\, t_0$$

$$\cong \frac{1}{t_0} \int_0^{t_0} v^2(t_0)\, d\, t_0$$

$$\cong v_{rms} \qquad (3.12)$$

showing that the root mean square velocity is measured in slant frames in the same sense that it is measured in standard coordinates.

Interpretation Coordinates in Stratified Media

The concept of interpretation coordinates was introduced in the previous chapter. The horizontal interpretation coordinate, x is earth-based and permits us to display data with a common reflection point (for non-dipping reflectors). This performs the same function as the transformation to common midpoint coordinates from common shot or geophone gathers. We now give the transformation from slant frame coordinates to interpretation coordinates for a depth-dependent velocity.

The horizontal interpretation coordinate was given in Chapter 2 as

$$x = x' - \Delta x(z) \qquad (2.11)$$

where Figure 2.13 shows that Δx is identical to $f/2$, the half-offset.

The previous section on root mean square velocity derived an expression for the offset as

$$f(z) = 2 \int_0^z \tan\theta(z)\, dz \tag{3.9}$$

$$= \int_0^{t_0} \frac{p\, v^2(t_0)\, d\, t_0}{(1-p^2 v^2(t_0))^{1/2}} \tag{3.10}$$

so, since $\Delta x(z) = f(z) / 2$, we have

$$x = x' - \int_0^z \tan\theta(z)\, dz$$

$$= x' - \frac{1}{2} \int_0^{t_0} \frac{p\, v^2\, (t_0)\, d\, t_0}{(1-p^2 v^2(t_0))^{1/2}} \tag{3.13}$$

which gives the transformation equation for the horizontal interpretation coordinate which we would like to express in terms of t' rather than t_0 .

Turning our attention momentarily to the interpretation time coordinate transformation, we write from Figure 3.4

$$d\, t_0 = \frac{2\, dz}{v(z)} = \cos\theta\ dt \tag{3.14}$$

where we recognize that θ is a function of depth. We have also that

$$t = t' + f\, p$$

and

$$dt = dt' + p\ df \tag{3.15}$$

since by staying on a ray path $dp = 0$. Therefore,

$$d t_0 = \cos\theta [\, dt' + p\, df \,]$$

and

$$d t_0 = \cos\theta [\, dt' + \cos\theta \sin\theta \tan\theta\, d t_0 \,]$$

having used equation (3.10).

Simplifying,

$$(1 - \sin^2\theta)\, d t_0 = \cos\theta\, dt'$$

or

$$t_0 = \int_0^{t'} \frac{dt'}{\cos\theta(p,t')}$$

$$= \int_0^{t'} \frac{dt'}{(1-p^2v^2(p,t'))^{1/2}} \qquad (3.16a)$$

which is the desired transformation for the time coordinate $t' \rightarrow t_0$.

Incorporating (3.16a) into (3.13) gives the desired horizontal transformation.

$$x = x' - \frac{1}{2} \int_0^{t'} \frac{pv^2(p,t')dt'}{(1-p^2v^2(p,t'))} \qquad (3.16b)$$

Equations (3.16) embody the interpretation coordinate transformation $(x',t') \rightarrow (x,t_0)$ in a stratified media $v = v(z)$.

The results of the previous section allow us to express (3.16) in terms of an rms velocity if we choose to make the straight line ray path assumption

$$x = x' - \frac{p\, v_{rms}^2(p,t')\, t'}{2(1-p^2 v_{rms}^2(p,t'))} \tag{3.17a}$$

and

$$t_0 = \frac{t'}{(1-p^2 v_{rms}^2(p,t'))^{1/2}} \tag{3.17b}$$

Recall that the transformation to interpretation coordinates (x,t_0) require an exact knowledge of the depth-dependent velocity, $v(z)$. If only an approximate velocity is available $\hat{v}(z)$, then we have a transformation to approximate interpretation coordinates, $(\hat{x},\ \hat{t}_0)$.

$$\hat{x} = x' - \int_0^{t'} \frac{p\, \hat{v}^2(p,t')\, dt'}{(1-p^2\hat{v}^2(p,t'))} \tag{3.18a}$$

$$\hat{t}_0 = \int_0^{t'} \frac{dt'}{(1-p^2\hat{v}^2(p,t'))^{1/2}} \tag{3.18b}$$

Let us now summarize the scheme which we have implied in this section to estimate velocities using interpretation coordinates. We have slant frame data in $(x',\ p,\ t')$ coordinates with no velocity information.

We wish to pick a trial rms velocity, $\hat{v}$, for which we will measure coherency along some trajectory which it predicts in order to compare its closeness to the true velocity. Begin by picking some value of the approximate interpretation coordinate $\hat{x}$, say $\hat{x} = \hat{x}_0$, which will be held fixed. Then for some trial rms velocity, $\hat{v}$, and

for some time point, $\hat{t}_0$, defined at $p = 0$, we have the trajectory defined in (x', p, t') space to be

$$x' = \hat{x}_0 - \frac{p\,\hat{v}^2\,t'}{2(1-p^2\hat{v}^2)} \tag{3.19a}$$

$$= \hat{x}_0 - \frac{p\,\hat{v}^2\,\hat{t}_0}{2(1-p^2\hat{v}^2)^{1/2}} \tag{3.19b}$$

$$p = p$$

$$t' = \hat{t}_0\,(\,1 - p^2\,\hat{v}^2\,)^{1/2} \tag{3.19c}$$

with p chosen as the independent variable.

Note that the transformation of (3.19) changes with each new trial velocity $\hat{v}$. Equivalently, for a single choice of $\hat{x}_0$ and $\hat{t}_0$, each value of $\hat{v}$ defines a unique trajectory in (x', p, t') space.

Estimation of Interval Velocities in Slant Frames

If two reflectors exist, one at depth z_1 , and one at $z_1 + \Delta z$ we would like to be able to make an estimate of the velocity in the interval Δz directly from the data. Let us assume that in the region $z < z_1$ the velocity is an arbitrary function of depth only; i.e., $v = v(z) \neq v(x,z)$. We further assume that in the interval Δz the velocity is constant; i.e., $v(z_1) \equiv v_1 = \text{constant}$. If Δz is so large that the assumption of a constant velocity is poor, then the results of an earlier section let us claim that any velocity which we measure shall be the root mean square velocity for the interval.

Figure 3.3 shows ray paths for two horizontal reflectors in a slant frame. The two downgoing ray paths are through an arbitrarily depth-dependent velocity, but will at all depths be parallel because all downgoing energy has the same ray parameter, p .

We write for the reflector at z_1

$$t_1' = t_1 - f_1 p \tag{3.20}$$

where, as before, t' is the slant frame time coordinate and t is the shot to geophone time. We now write the above equation for the reflector at $z_1 + \Delta z$,

$$(t_1' + \Delta t') = (t_1 + \Delta t) - (f_1 + \Delta f) p \tag{3.21}$$

and subtracting the two equations,

$$\Delta t' = \Delta t - p \, \Delta f \tag{3.22}$$

Now we have from the geometry of Figure 3.3,

$$\Delta t = \frac{2 \, \Delta z}{v_1 \cos \theta_1} \tag{3.23a}$$

and

$$\Delta f = 2 \, \Delta z \tan \theta_1 \tag{3.23b}$$

where $\theta_1 \equiv \theta(z_1)$.

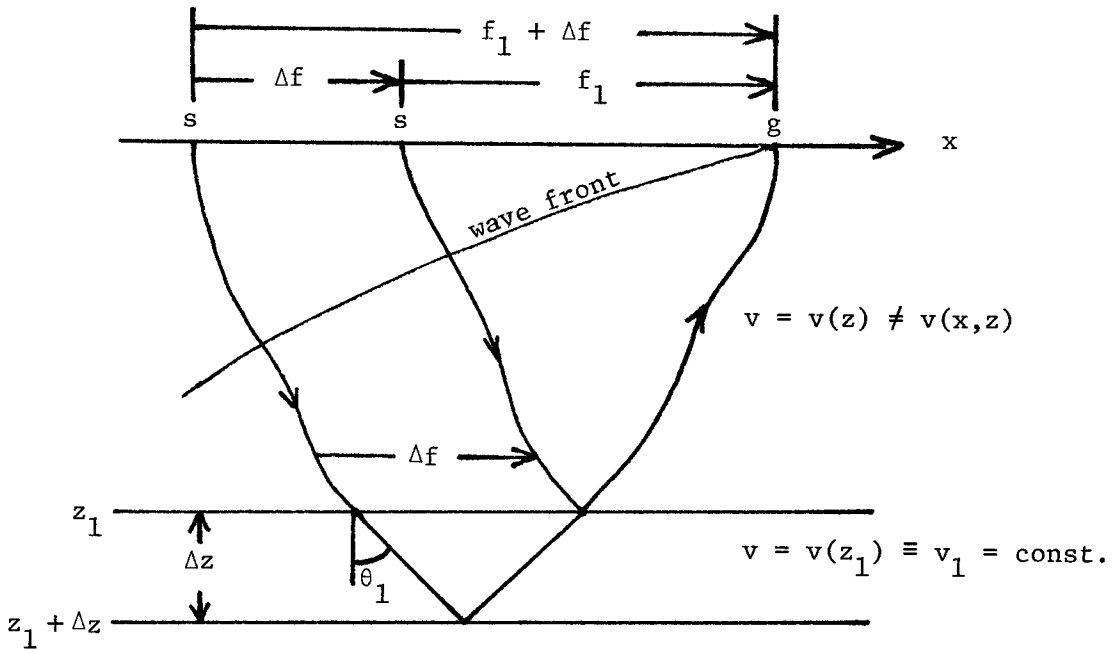

Figure 3.3. Ray diagram in slant frames for interval velocity estimation. Depth-dependent velocity above z_1 arbitrary but independent of x. Differences in slant frame arrival times at various values of p allow interval velocity estimation. See figure below.

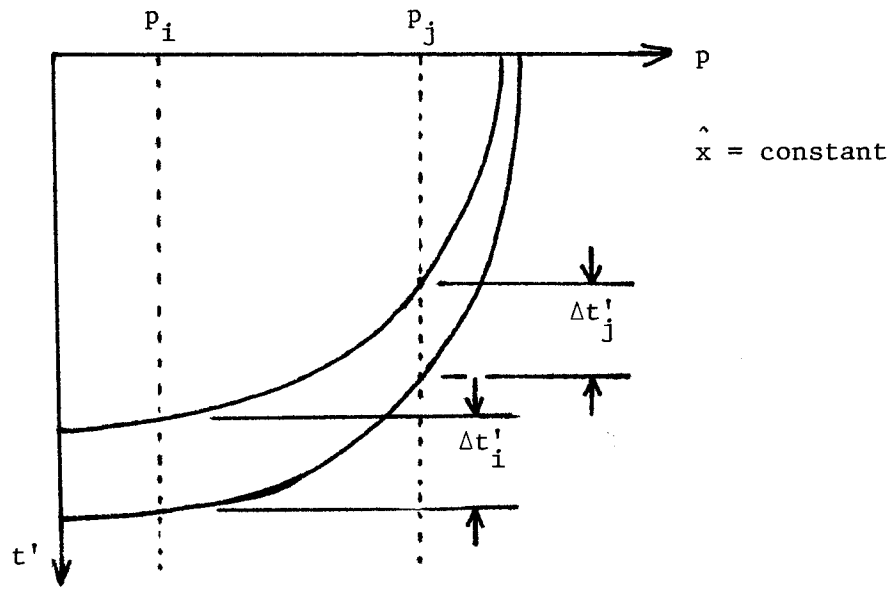

Figure 3.4. Two events on a p-gather which may be used to estimate the interval velocity between them. The data in this gather should be at a constant value of the approximate interpretation coordinate, $\hat{x}$.

Combining equations (3.23) with (3.22) gives

$$\Delta t' = \frac{2\,\Delta z}{v_1 \cos\theta_1} - 2\,p\,\Delta z \tan\theta_1$$

$$= \frac{2\,\Delta z \cos\theta_1}{v_1} \qquad (3.24)$$

by trigonometric identity.

Now rewrite (3.24) twice for two different values of p .

$$\Delta t'_i = \frac{2\,\Delta z}{v_1} \left[1 - p_i^2 v_1^2 \right]^{1/2} \qquad (3.25a)$$

and

$$\Delta t'_j = \frac{2\,\Delta z}{v_1} \left[1 - p_j^2 v_1^2 \right]^{1/2} \qquad (3.25b)$$

then dividing (3.25a) by (3.25b),

$$\frac{\Delta t'_i}{\Delta t'_j} = \left[\frac{1 - p_i^2 v_1^2}{1 - p_j^2 v_1^2} \right]^{1/2} \qquad (3.26)$$

or by rearranging the equation,

$$v_1 = \left[\frac{\Delta t'^2_i - \Delta t'^2_j}{p_j^2 \Delta t'^2_i - p_i^2 \Delta t'^2_j} \right]^{1/2} \qquad (3.27)$$

which gives an expression for the interval velocity, v_1 , as a function of the time intervals $\Delta t'_i$ and $\Delta t'_j$ for two values of p , p_i and p_j . Figure 3.4 shows the relationship among the parameters.

More values of p than two can be accommodated into an expression like (3.27) by considering them to be redundant information and using a method such as least squares. However, in the field data example in this chapter, six values of p were available, but only

two showed the reflections clearly. In other situations, severely angle-dependent reflection coefficients may result in only a few values of p showing clear reflections, and thus a simple equation like (3.27) may often be the method of choice.

In many cases we will wish to make measurements of the time intervals $\Delta t'$ such that they represent reflections from a common depth point for flat reflectors. This is desirable, for example, when reflectors show poor lateral continuity, or to make a first order correction when gentle dips are present. (Higher order corrections, requiring migration, will be discussed in Chapter 4.) We therefore wish to measure $\Delta t'$ for all values of p for a fixed value of x. Since, the transformation $x' \leftrightarrow x$ can be done exactly only with perfect knowledge of the depth-dependent velocity, we must use a velocity estimate for an approximate transformation $x' \leftrightarrow \hat{x}$ in order to make a first measurement of the time intervals $\Delta t'$. The resultant velocity can then be used in a new transformation $x' \leftrightarrow \hat{x}$ and subsequently to a refined velocity estimate.

Four values of x' must be calculated for each of the two reflectors at each of two values of p. x' can be calculated from a transposition of the previously derived interpretation coordinate transformation

$$x' = \hat{x}_0 + \frac{p}{2} \int_0^{t'} \frac{\hat{v}^2(p,t')\, dt'}{(1-p^2\hat{v}^2(p,t'))} \tag{3.28}$$

where $\hat{x}_0$ is fixed.

It appears from equation (3.28) that the value of t' must be known in order to make the transformation. Again, an approximate value must be introduced into the transformation. The assumption that is being implicitly made in this derivation is that the reflector dips will be low enough so that any $\Delta t'$ measured from the data will be only weakly dependent on x' .

A Synthetic Data Example

Figure 3.5 and 3.6 show a synthetic common geophone gather and the p-gather that was created from it. The noise was obtained from field data so that it would have normal spectral characteristics.

The events on the gather appear at half-second intervals beginning at $t_0 = .4$ seconds, and all have a characteristic velocity of 5700 ft/sec. The waveforms used were symmetric with no d.c. component, and the dominant wave length sampled at about 8 points per wavelength. The sample interval was 4 milliseconds. The waveforms are identical and of equal strength everywhere on the common geophone gather.

The slant stack was done using the end effect reduction and anti-aliasing scheme described in Appendix A. The stacking velocity was 5700 ft/sec and the $\Delta\theta$ parameter was $30°$.

A significant improvement in signal to noise is seen on the p-gather. This is consistent with the claim made in the previous chapter that the slant stack is a partial coherency stack.

Figure 3.6 shows the mute which was applied to the p-gather. This allowed us to keep only those regions of the gather in which real coherent energy was present. Close examination also shows that the

noise is somewhat coherent from trace to trace in the p-gather, indicating that we are apparently over-sampled in p-space.

Figure 3.7 shows the velocity profile using all the data in both frames (after the mute in the case of the slant frame). The coherency measure, $c(t_0, v)$, was a partially normalized sum over each trajectory (a hyperbola in the case of the standard geometry, and an ellipse in the case of the slant frame).

$$c(t_0,v) = \frac{\sum_{t_0-\delta t/2}^{t_0+\delta t/2} \left[\sum_{\text{trajectory}} P \right]^2}{\left[\sum_{t_0-\delta t/2}^{t_0+\delta t/2} \sum_{\text{trajectory}} P^2 \right]^{1/2}} \qquad (3.29)$$

where P is the data in either frame (i.e., $P(f,t)$ or $P(p,t')$). The outer time gate, δt, was 10 milliseconds.

Figure 3.7 shows that we can expect to make a velocity estimate in the slant frame, but we appear to have raised the noise level in the velocity profile somewhat.

Figure 3.8 shows velocity profiles for the two data displays having used only 5 traces, equally spaced, in each coherency summation. In this comparison the overall noise level appears to be higher for the standard geometry.

We conclude from this trial with the synthetic data example that

1) a velocity estimation can be done in slant frames,

2) when using all traces in standard geometry and a similar number in slant frames, the signal to noise ratio in the velocity profile is comparable in the two methods, and

3) when using only a few traces in the velocity estimate, the slant frames appear to give a higher signal to noise ratio.

A Field Data Example

A previous section of this chapter discussed the calculation of interval velocity, and determined that the velocity in the region between two reflectors could be calculated from data stacked over a minimum of two values of p. We will use this result to estimate an interval velocity from the field data of Chapter 2.

Figures 2.16 and 2.17 show slant sections for $p = 0.03$ msec/ft and 0.05 msec/ft. At approximately 2.5 seconds an event can be seen on each section, labeled "event", which is not apparent on the CMP stacked section (Figure 2.14). This is evidently very angle-dependent primary energy, since it cannot be seen on any of the other four slant sections. We shall calculate the velocity between this event and the sea floor primary.

The necessary relation derived earlier for two values of p is

$$v_1 = \left[\frac{\Delta t_i'^2 - \Delta t_j'^2}{p_j^2 \Delta t_i'^2 - p_i^2 \Delta t_j'^2} \right]^{1/2} \qquad (3.27)$$

where the interval velocity, v_1, is taken to be constant. Application of (3.27) is straightforward, but we need to determine at what value of the horizontal coordinate, x', the arrival times, t', should be measured.

For a first guess at the horizontal transformation $x' \leftrightarrow x$, we will choose that which the data has already undergone before plotting, i.e., using water velocity. If v_w is water velocity (taken to be equal to 5000 ft/sec), then the horizontal transformation $x' \leftrightarrow x_w$ that the data has undergone is given by

$$x_w = x' - \frac{p}{2}\int_0^{t'} \frac{v_w^2\, dt'}{(1-p^2v_w^2)} \qquad (3.30)$$

$$= x' - \frac{p\, v_w^2\, t'}{2(1-p^2v_w^2)}$$

and we will make all measurements of $\Delta t'$ at some x_w = constant. Since we have no horizontal scale on Figures 2.16 and 2.17, we have taken x_w = constant to be that trace at which the dead shot intercepts $t' = 0$ (note that $x_w = x'$ at $t' = 0$) . Figure 3.9 shows this schematically.

Now we are prepared to make a first measurement of time intervals. We wish to obtain the intervals $\Delta t'$, but the time scales in the figures have also been transformed at water velocity according to

$$t_w = \frac{t'}{(1-p^2v_w^2)^{1/2}} \qquad (3.31)$$

Since we will measure Δt_w , we rewrite equation (3.27)

$$v_1 = \left[\frac{\Delta t'^2_i - \Delta t'^2_j}{p_j^2\Delta t'^2_i - p_i^2\Delta t'^2_j}\right]^{1/2} \qquad (3.27)$$

$$= \left[\frac{\Delta t^2_{w,i}(1-p_i^2v_w^2) - \Delta t^2_{w,j}(1-p_j^2v_w^2)}{p_j^2\Delta t^2_{w,i}(1-p_i^2v_w^2) - p_i^2\Delta t^2_{w,j}(1-p_j^2v_w^2)}\right]^{1/2} \qquad (3.32)$$

$$= \left[\frac{(.9775)\Delta t^2_{w,i} - (.9375)\Delta t^2_{w,j}}{(.9775)(.00005\text{sec/ft})^2\Delta t^2_{w,i} - (.9375)(.00003\text{sec/ft})^2\Delta t^2_{w,j}}\right]^{1/2}$$

where p_i is taken to be .03 msec/ft and p_j = .05 msec/ft.

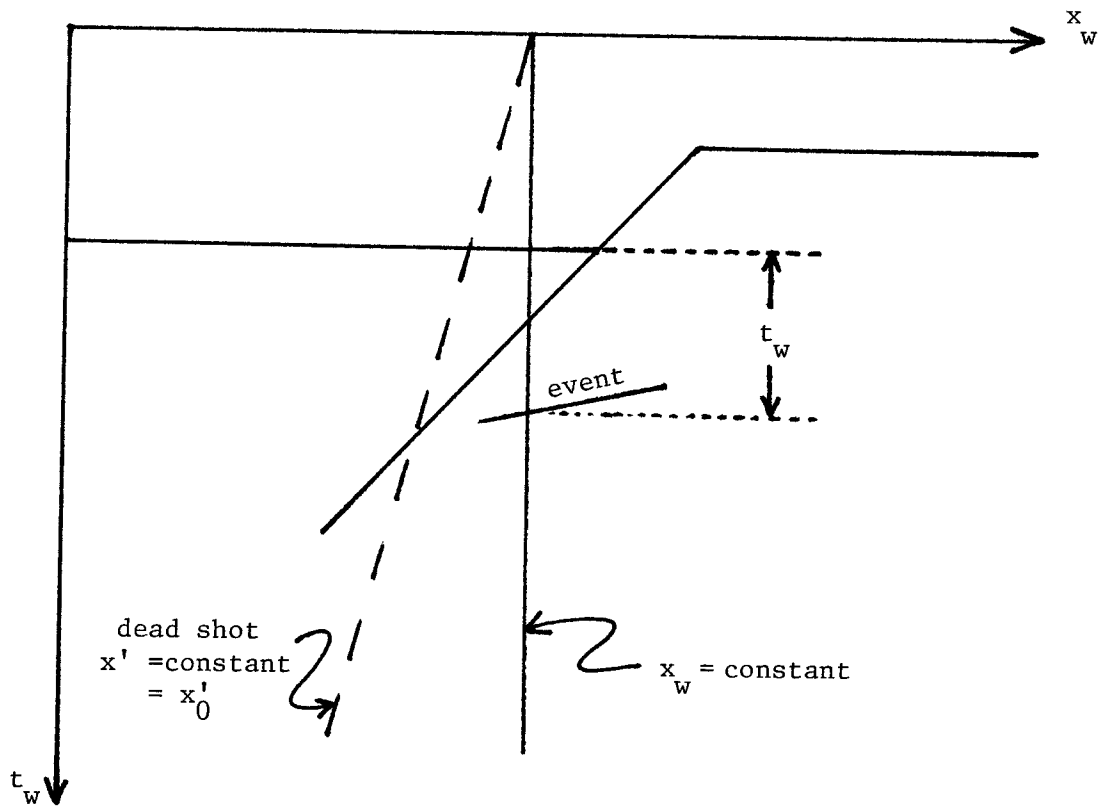

Figure 3.9. A schematic representation of slant sections of Figures 2.16 and 2.17. The horizontal and vertical scales have already been transformed using water velocity from (x',t') to (x_w,t_w). We wish to measure $\Delta t'$ at a fixed value of x, but as a first guess we measure Δt_w at a fixed value of x_w, as shown. The figure shows that the value of x_w chosen is such that a particular "dead shot" trace intercepts it at $t_w = 0$. The interval Δt_w is then converted to the desired interval, $\Delta t'$, by the transformation

$$\Delta t' = \Delta t_w (1 - p^2 v_w^2)^{1/2}$$

where v_w = 5000 ft/sec.

Measurement of Δt_w yielded 1.07 sec and 0.92 sec for the i and j sections respectively, leading to a first guess interval velocity

$$v_1 = 12{,}600 \text{ ft/sec}$$

For the correction to the x-shifting, we incorporate the above value for v_1 into the integral

$$x' = \hat{x} + \frac{p}{2} \int_0^{t'} \frac{\hat{v}^2(t')dt'}{1-p^2\hat{v}^2(t')}$$

$$= \hat{x} + \frac{p\, v_w^2 (t'_{\text{sea floor}})}{2(1-p^2 v_w^2)} + \frac{p\, v_1^2 (t'_{\text{event}} - t'_{\text{sea floor}})}{2(1-p^2 v_1^2)}$$

This correction on the x-shift allows a second estimate of the velocity to be made.

The new values for Δt_w are

$$\Delta t_w = \begin{cases} 1.03 \text{ sec} & \text{for } p = .03 \text{ msec/ft} \\ 0.80 \text{ sec} & \text{for } p = .05 \text{ msec/ft} \end{cases}$$

where we had to pick a new fixed value for $\hat{x}$, so that the new shifted horizontal position would be within the finite lateral extent of the event. This yielded a new velocity estimate of

$$v_1 = 14{,}600$$

which differs from the first estimate by 16%. The 16% correction is somewhat large because the event is dipping.

The refined estimate of v_1 is perhaps unreasonably high and suggests the question of whether or not the event is indeed primary energy. The propagating angles in the region with velocity v_1 become 26° and 47° for the smaller and larger p values respectively.

Although the values are large, they are far from approaching critical angle.

The interval velocity calculations were done using theory developed for horizontal layering. To estimate the perturbing effect of the dip of the event in question on the velocity estimate, we borrow a result from the next chapter. For an event of dip ϕ, the travel time curve in slant frames will be

$$\frac{t'}{t'_0} = \cos(\theta + \phi) \tag{4.1}$$

where t'_0 is the zero offset two-way travel time from some datum and at a fixed horizontal-coordinate (earth-based). The datum shall be the sea floor.

An interval velocity relation can be developed with the help of (4.1) in a parallel manner to the treatment of horizontal layers. We use (4.1) to write a generalized form of equation (3.26)

$$\frac{\Delta t'_i}{\Delta t'_j} = \frac{\cos(\theta_i + \phi)}{\cos(\theta_j + \phi)} \tag{3.33}$$

$$= \frac{\cos\theta_i \cos\phi - \sin\theta_i \sin\phi}{\cos\theta_j \cos\phi - \sin\theta_j \sin\phi}$$

$$= \frac{(1 - p_i^2 v_1^2)^{1/2} \cos\phi - p_i v_1 \sin\phi}{(1 - p_j^2 v_1^2)^{1/2} \cos\phi - p_j v_1 \sin\phi}$$

or

$$\frac{\Delta t'_i}{\Delta t'_j} = \frac{(1 - p_i^2 v_1^2)^{1/2} - p_i v_1 \tan\phi}{(1 - p_j^2 v_1^2)^{1/2} - p_j v_1 \tan\phi} \tag{3.34}$$

which is a transcendental equation in v_1 with all parameters known except dip ϕ. The dip of the event was estimated from the two slant sections assuming them to be zero offset sections when displayed in (x_w, t_w) coordinates. With the refined estimate of v_1 used, the dip was calculated to be

$$\phi = \begin{cases} 15.7° & \text{for } p = 0.05 \text{ msec/ft} \\ 15.2° & \text{for } p = 0.03 \text{ msec/ft} \end{cases}$$

A final value of

$$\phi = 14.5°$$

was chosen as an extrapolation of the two above values to $p = 0$.

With the above value for ϕ entered into the transcendental equation (3.34), v_1 was calculated to be

$$v_1 = 14{,}300$$

which is in good agreement with the second iteration using the theory for horizontal layers.

Figure 3.10 shows CMP gathers for the far right region of the section where the sea floor primary arrives at approximately 0.4 seconds. The geophone group spacing is 220 ft and the critically refracted energy shows a characteristic velocity of 13,000 ft/sec. Although this is somewhat smaller than our second iteration estimate for the interval velocity, it is at a shallower depth of burial and at least suggests higher velocities than one normally may expect.

The above calculations seem to confirm that the "event" was indeed genuine primary energy, and has served to demonstrate our method of interval velocity estimation from slant sections. In the case where energy from reflectors is angle-dependent, this method permits taking advantage of the selective illumination angle characteristic of slanted plane wave sections.